

BRIEF COMMUNICATIONS

Dogs cloned from adult somatic cells

Two Afghan pups could help to unravel the genetics behind the assorted traits of other canine breeds.

Several mammals — including sheep, mice, cows, goats, pigs, rabbits, cats¹, a mule², a horse³ and a litter of three rats⁴ — have been cloned by transfer of a nucleus from a somatic cell into an egg cell (oocyte) that has had its nucleus removed. This technology has not so far been successful in dogs because of the difficulty of maturing canine oocytes *in vitro*. Here we describe the cloning of two Afghan hounds by nuclear transfer from adult skin cells into oocytes that had matured *in vivo*. Together with detailed sequence information generated by the canine-genome project^{5,6}, the ability to clone dogs by somatic-cell nuclear transfer should help to determine genetic and environmental contributions to the diverse biological and behavioural traits associated with the many different canine breeds^{7,8}.

Successful somatic-cell nuclear transfer (SCNT) depends on the quality, availability and maturation of the animal's unfertilized oocytes. Unlike other mammals, dogs ovulate at first meiotic prophase, and their oocytes mature for 2 to 3 days in the oviduct's distal regions. Previously, intra- and interspecific canine embryos have been constructed by canine SCNT into canine and bovine oocytes, respectively, but this did not result in viable offspring⁹.

We collected oocytes matured *in vivo* at metaphase II about 72 hours after ovulation by flushing the oviducts. (For details of methods, see supplementary information.) Donor fibroblasts were obtained from an ear-skin biopsy of a male Afghan hound and cultured for two to five passages (in which fully grown cells are transferred to a new culture dish). For SCNT, the chromosomes of the unfertilized canine oocytes were removed by micromanipulation, and a single donor cell was transferred into each enucleated oocyte. The couplets were fused and only successfully fused couplets (75%) were activated. The activated oocytes were then transferred into the oviducts or uterine horns of recipient dogs at times appropriate to the embryos' developmental stages. We collected an average of 12 oocytes from each female, and a total of 1,095 reconstructed canine embryos were transferred into 123 recipients.

Three pregnancies were confirmed by ultrasound scans at 22 days' gestation in recipients after transfer of constructs. Pregnancy was established only after embryo transfer of very-early-stage nuclear-transfer constructs (that is,



Figure 1 | Dog cloned by somatic-cell nuclear transfer. **a**, Snuppy, the first cloned dog, at 67 days after birth (right), with the three-year-old male Afghan hound (left) whose somatic skin cells were used to clone him. Snuppy is genetically identical to the donor Afghan hound. **b**, Snuppy (left) was implanted as an early embryo into a surrogate mother, the yellow Labrador retriever on the right, and raised by her.

less than 4 hours after oocyte activation). This transfer of early-stage embryos is a crucial factor in successful assisted reproductive technology for dogs. One fetus miscarried and two others were carried to term.

We named the first cloned dog Snuppy (for Seoul National University puppy); it is shown in Fig. 1a with the male Afghan fibroblast donor. Snuppy was delivered by caesarian section after 60 days (full term) from a yellow Labrador surrogate mother (Fig. 1b); his birth weight was 530 g. The second SCNT dog, NT-2, was carried by a mixed-breed surrogate, and was also delivered at 60 days, weighing 550 g (normal range for Afghans in a litter, 482–680 g). He experienced neonatal respiratory distress during the first week, seemed to recover, but died on day 22 as a result of aspiration pneumonia; no major anatomical anomalies were evident post mortem.

We tested whether the cloned dogs were genetically identical by microsatellite analysis of genomic DNA from the donor Afghan, the cloned dogs and the surrogates (see supplementary information). Analysis of eight canine-specific microsatellite loci confirmed that the cloned dogs were genetically identical to their donor dog. However, the efficiency of cloning is still very low (2 dogs from 123 recipients, or 1.6%) compared with the rates for cats¹ and horses³.

In addition to the benefits that cloning technology may generally provide (the preservation of rare species and therapeutic cloning

— once canine embryonic stem cells become available), this technology could become a useful research tool for studying the genetics of outcrossed populations.

Byeong Chun Lee*, **Min Kyu Kim***, **Goo Jang***, **Hyun Ju Oh***, **Fibrianto Yuda***, **Hye Jin Kim***, **M. Hossein Shamim***, **Jung Ju Kim***, **Sung Keun Kang***, **Gerald Schatten†**, **Woo Suk Hwang***

*Department of Theriogenology and Biotechnology, College of Veterinary Medicine, Seoul National University, Gwanak-gu, Seoul 151-742, South Korea
e-mail: hwangws@snu.ac.kr

†Pittsburgh Development Center, Magee-Womens Research Institute, Departments of Obstetrics–Gynecology–Reproductive Sciences and Cell Biology–Physiology, University of Pittsburgh School of Medicine, Pittsburgh, Pennsylvania 15213, USA

1. Shin, T. *et al. Nature* **415**, 859 (2002).
2. Woods, G. L. *et al. Science* **301**, 1063 (2003).
3. Galli, C. *et al. Nature* **424**, 635 (2003).
4. Zhou, Q. *et al. Science* **302**, 1179 (2003).
5. Ostrander, E. A. & Giniger, E. *Am. J. Hum. Genet.* **61**, 475–480 (1997).
6. Sutter, N. B. & Ostrander, E. A. *Nature Rev. Genet.* **5**, 900–910 (2004).
7. Lohi, H. *et al. Science* **307**, 81 (2005).
8. Modiano, J. F. *et al. Cancer Res.* **65**, 5654–5661 (2005).
9. Westhusin, M. E. *et al. J. Reprod. Fert. Suppl.* **57**, 287–293 (2001).

Supplementary information accompanies this communication on Nature's website.

Competing financial interests: declared none.
doi:10.1038/436641a

Unit, Institut Pasteur, 75724 Paris Cedex 15, France
e-mail: prangish@pasteur.fr

† University of Regensburg, 93053 Regensburg,
Germany

‡ Danish Archaea Centre, Institute of Molecular
Biology and Physiology, Copenhagen University,
1307 Copenhagen K, Denmark

1. van Regenmortel, M. H. V. in *Seventh Report of the International Committee on Taxonomy of Viruses* (eds Fauquet, C. M. et al.) 3–16 (Academic, San Diego, 2000).
2. Lupas, A., Van Dyke, M. & Stock, J. *Science* **252**, 1162–1164 (1991).
3. Strelkov, S. V., Herrmann, H. & Aebi, U. *BioEssays* **25**, 243–251 (2003).
4. Ausmess, N., Kuhn, J. R. & Jacobs-Wagner, C.

Cell **115**, 705–713 (2003).

5. Herrmann, H. & Aebi, U. *Curr. Opin. Cell Biol.* **12**, 79–90 (2000).
6. Pettit, S. C., Everitt, L. E., Choudhury, S., Dunn, B. M. & Kaplan, A. H. *J. Virol.* **78**, 8477–8485 (2004).
7. Swanstrom, R. & Willis, J. W. in *Retroviruses* (eds Coffin, J. M., Hughes, S. H. & Varmus, H. E.) 263–334 (Cold Spring Harbor Lab. Press, New York, 1997).
8. Ackermann, H. W. & Bamford, D. in *Seventh Report of the International Committee on Taxonomy of Viruses* (eds Fauquet, C. M. et al.) 111–116 (Academic, San Diego, 2000).
9. Prangishvili, D., Stedman, K. & Zillig, W. *Trends Microbiol.* **9**, 39–43 (2001).

Supplementary information accompanies this communication on Nature's website.

Competing financial interests: declared none.

doi:10.1038/nature4361101a

GREEN CHEMISTRY

Reversible nonpolar-to-polar solvent

Imagine a smart solvent that can be switched reversibly from a liquid with one set of properties to another that has very different properties, upon command. Here we create such a system, in which a non-ionic liquid (an alcohol and an amine base) converts to an ionic liquid (a salt in liquid form) upon exposure to an atmosphere of carbon dioxide, and then reverts back to its non-ionic form when exposed to nitrogen or argon gas. Such switchable solvents should facilitate organic syntheses and separations by eliminating the need to remove and replace solvents after each reaction step.

Chemical production processes often involve multiple reaction and separation steps, and the type of solvent that is optimum for a particular step may be different from the one needed in the next step. The solvent is therefore usually removed after each step and a new solvent added in preparation for the next, significantly adding to the economic cost and environmental impact of the process. This cumbersome procedure would be unnecessary if a solvent's properties could be adjusted for the following step while still in the reaction vessel, enabling the same solvent to be used for several consecutive reaction or separation steps. Moderate changes in temperature and pressure are incapable of triggering significant changes in the properties of conventional solvents. In contrast, supercritical fluids¹ and CO₂/organic solvent mixtures² can be modified by pressure changes, but unfortunately only above 40 bar.

The reaction we describe reversibly changes the nature and properties of a solvent but occurs under very mild conditions. We reasoned that switching a normal non-ionic liquid to an ionic liquid should induce a change in its properties: ionic liquids are often viscous and always polar, whereas non-ionic solvents are typically non-viscous and vary widely in polarity. We chose CO₂ as the 'switch' to elicit this change because it is a benign agent

and easily removed. (For methods, see supplementary information.)

We found that exposure of a 1:1 mixture of the two non-ionic liquids, namely DBU (1,8-diazabicyclo-[5.4.0]-undec-7-ene) and 1-hexanol, to gaseous CO₂ at one atmosphere and at room temperature causes conversion of the liquid mixture to an ionic liquid (Fig. 1a, b). This is readily converted back into a non-ionic liquid by bubbling N₂ or argon through

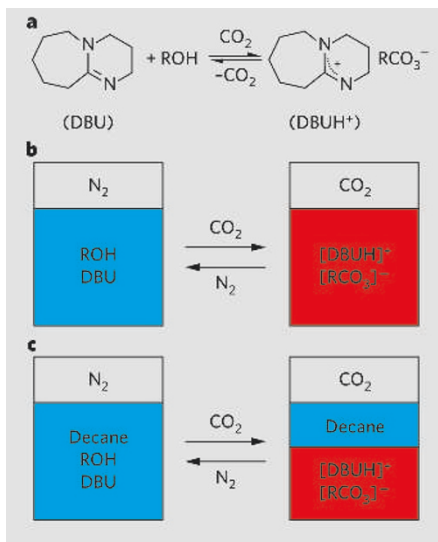


Figure 1 | The 'switching' of a switchable solvent.

a, Protonation of DBU (1,8-diazabicyclo-[5.4.0]-undec-7-ene) in the presence of an alcohol and carbon dioxide is reversed when CO₂ is removed. **b**, Polarity switching in the reaction shown in **a**, in which CO₂ causes a nonpolar liquid (shown in blue) mixture of hexanol and DBU to change over one hour into a polar, ionic liquid (shown in red); nitrogen gas reverses the process by stripping out CO₂ from the reaction. **c**, The different polarity of each liquid under the two conditions is illustrated by the miscibility of decane with the hexanol/DBU mixture under nitrogen, before exposure to CO₂; however, decane separates out once the mixture becomes polar in the presence of CO₂. Again, N₂ reverses the process.

the liquid at room temperature or, for a more rapid reaction, at 50 °C. These changes are demonstrated by chemical shifts in key protons, as revealed by ¹H-NMR spectroscopy, and by solvatochromic measurement of the polarity of the solvent before and after exposure to CO₂ (see supplementary information).

The reaction is exothermic and causes a marked increase in the viscosity of the liquid. The choice of alcohol is critical because the 1-hexylcarbonate salt (Fig. 1, right) is a viscous liquid at room temperature, whereas the bicarbonate^{3,4} and methylcarbonate (ref. 5, and A. D. Main, G. E. Fryxell and J. Linehan, unpublished results) salts are solids and so are not candidates for smart solvents.

Our non-ionic liquid is as nonpolar as chloroform, according to measurements using Nile Red as solvatochromic dye (see supplementary information), whereas the liquid under CO₂ is as polar as dimethylformamide or propanoic acid. The polarity changes in this switchable solvent system are demonstrated by testing the solubility of decane, a nonpolar compound, in each liquid: it is miscible with the liquid under N₂ but not with that under CO₂ (Fig. 1c). We conclude that N₂ and CO₂ at 1 bar can be used as triggers of miscibility and immiscibility, respectively.

We have built solvent switchability into molecules that are small enough to be liquid at room temperature. Further examples of switchable solvents, preferably ones less Lewis-basic than DBU, should eventually enable their application in the 'green' production of high-value chemicals such as pharmaceuticals.

Philip G. Jessop*, **David J. Heldebrant***,
Xiaowang Li*, **Charles A. Eckert†**, **Charles L. Liotta†**

*Department of Chemistry, Queen's University,
Kingston, Ontario K7L 3N6, Canada
e-mail: jessop@chem.queensu.ca

†Schools of Chemistry and Chemical Engineering,
Georgia Institute of Technology, Atlanta, Georgia
30332-0100, USA

1. Jessop, P. G. & Leitner, W. (eds) *Chemical Synthesis using Supercritical Fluids* (VCH/Wiley, Weinheim, 1999).
2. Subramaniam, B. & Busch, D. H. in *Carbon Dioxide Conversion and Utilization* (eds Song, C., Gaffney, A. F. & Fujimoto, K.) 364–386 (ACS, Washington, 2002).
3. Perez, E. R. et al. *J. Org. Chem.* **69**, 8005–8011 (2004).
4. Heldebrant, D. J., Jessop, P. G., Thomas, C. A., Eckert, C. A. & Liotta, C. L. *J. Org. Chem.* **70**, 5335–5338 (2005).
5. Munshi, P., Main, A. D., Linehan, J., Tai, C. C. & Jessop, P. G. *J. Am. Chem. Soc.* **124**, 7963–7971 (2002).

Supplementary information accompanies this communication on Nature's website.

Competing financial interests: declared none.

doi:10.1038/nature4361102a

Corrigendum

Dogs cloned from adult somatic cells

Byeong Chun Lee, Min Kyu Kim, Goo Jang, Hyun Ju Oh, Fibrianto Yuda, Hye Jin Kim, M. Hossein Shamin, Jung Ju Kim, Sung Keun Kang, Gerald Schatten, Woo Suk Hwang *Nature* **436**, 641 (2005)

This communication contains an error in the methods section of the supplementary information. In the description of the fusion protocol on page 3, line 2, electrical pulses were delivered for 15 microseconds, and not for 15 seconds as published.

GAMMA-RAY BURSTS

Huge explosion in the early Universe

Long gamma-ray bursts (GRBs) are bright flashes of high-energy photons that can last for tens of minutes; they are generally associated with galaxies that have a high rate of star formation and probably arise from the collapsing cores of massive stars, which produce highly relativistic jets (collapsar model¹). Here we describe γ - and X-ray observations of the most distant GRB ever observed (GRB 050904): its redshift^{2,3} (z) of 6.29 means that this explosion happened 12.8 billion years ago, corresponding to a time when the Universe was just 890 million years old, close to the reionization era⁴. This means that not only did stars form in this short period of time after the Big Bang, but also that enough time had elapsed for them to evolve and collapse into black holes.

GRB 050904 triggered the Burst Alert Telescope (BAT) on board the Swift⁵ satellite on 4 September 2005 at 1:51:44 GMT. The spacecraft quickly slewed to allow observations by

the X-ray Telescope (XRT)^{6,7}, which measured the burst for ten days after its onset. Figure 1 (top panel) shows the history of the burst. We shall present and discuss the GRB phenomenology from the point of view of the rest frame of its source.

The BAT light curve shows three main peaks: two of about 2 s at $T + 3.8$ s and $T + 7.7$ s, and a long-lasting one at about $T + 13.7$ s, where T is the time of the burst onset. It also shows a weak peak at about $T + 64$ s. The early XRT light curve shows a steep power-law decay with an index of -2.07 ± 0.03 ; two flares are superimposed at $T + 64$ s (coincident with the last peak of the BAT light curve) and $T + 170$ s. Although interrupted by the constraints of low-Earth-orbit observation, the X-ray light curve reveals highly irregular intensity variations, probably due to the presence of flares for up to $T + 1.5$ hours. At later times, flaring activity is not detected, leaving only a residual emission that is 10^6 times lower than the initial intensity.

The flares in the XRT light curve can be interpreted as late internal shocks related to central engine activity. In this scenario, they would have the same origin as the first γ -ray emission^{8–10}, which would require the central engine to remain active for at least 5,000 seconds, consistent with the collapsar model¹.

Spectral analysis was performed by selecting time intervals corresponding to characteristic phases of the light curve evolution. All spectra were well modelled by a single power law, with both galactic and intrinsic absorption components in the case of the XRT spectra. Figure 1 (bottom) shows the evolution with time of the photon index Γ . The BAT spectra have $\Gamma = -1.2$. If we exclude the spectrum of the first XRT flare at $T + 64$ s, the XRT photon indices show a clear, decreasing trend from about -1.2 to about -1.8 in the first $T + 200$ s. No further spectral evolution is present in later XRT data.

The overall phenomenology of GRB 050904 is not peculiar with respect to other GRBs at lower redshift. This suggests that the mechanisms of GRB explosions in the early Universe and today are similar.

Based on the likely existence of population I/II stars in galaxies that were already metal-enriched at these high redshifts¹¹, we expect about 10% of all bursts detected by Swift to be located at $z \geq 5$. A higher percentage would require an additional contribution to the high-redshift GRB population by metal-free population III stars, which are viable GRB progenitors for long-duration GRBs¹¹. A more systematic search for GRB optical counterparts will increase the sample of these high-redshift GRBs, allowing us to probe the existence of metal-free massive stars of population III.

G. Cusumano¹, V. Mangano¹, G. Chincarini^{2,3}, A. Panaitescu⁴, D. N. Burrows⁵, V. La Parola¹,

T. Sakamoto^{6,7}, S. Campana², T. Mineo¹, G. Tagliaferri², L. Angelini⁶, S. D. Barthelémy⁶, A. P. Beardmore⁸, P. T. Boyd⁶, L. R. Cominsky⁹, C. Gronwall⁵, E. E. Fenimore⁴, N. Gehrels⁵, P. Giommi¹⁰, M. Goad⁸, K. Hurley¹¹, J. A. Kennea⁵, K. O. Mason¹², F. Marshall⁶, P. Mészáros^{5,13}, J. A. Nousek⁵, J. P. Osborne⁸, D. M. Palmer⁴, P. W. A. Roming⁵, A. Wells⁹, N. E. White⁶, B. Zhang¹⁴

¹INAF-Istituto di Astrofisica Spaziale e Fisica Cosmica di Palermo, 90146 Palermo, Italy
e-mail: cusumano@ifc.inaf.it

²INAF Osservatorio Astronomico di Brera, 23807 Merate, Italy; ³Università degli studi di Milano-Bicocca, Dipartimento di Fisica, 20126 Milan, Italy; ⁴Los Alamos National Laboratory, PO Box 16633, Los Alamos, New Mexico 87545, USA; ⁵Department of Astronomy & Astrophysics and ¹³Department of Physics, Pennsylvania State University, Philadelphia, Pennsylvania 16802, USA; ⁶NASA/Goddard Space Flight Center, Greenbelt, Maryland 20771, USA; ⁷National Research Council, T2114, Washington DC 20418, USA; ⁸Department of Physics and Astronomy, University of Leicester, Leicester LE1 7RH, UK; ⁹Department of Physics and Astronomy, Sonoma State University, Rohnert Park, California 94928-3609, USA; ¹⁰ASI Science Data Center, 00044 Frascati, Italy; ¹¹Space Sciences Laboratory, University of California, Berkeley, California 94720-7450, USA; ¹²Mullard Space Science Laboratory, University College London, Holmbury St Mary, Dorking, Surrey RH5 6NT, UK; ¹⁴Department of Physics, University of Nevada, Box 454002, Las Vegas, Nevada 89154-4002, USA

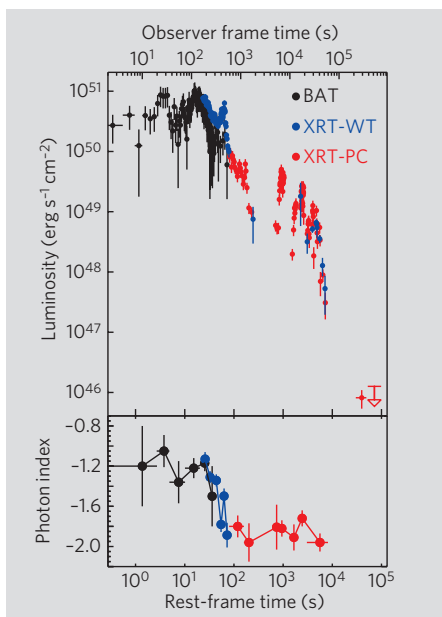


Figure 1 | Light curve and spectral evolution of GRB 050904 as observed by the Burst Alert Telescope (BAT) and the X-ray Telescope (XRT). WT, windowed timing mode data; PC, photon counting data. Top, evolution of the gamma-ray burst (GRB) K -corrected 0.2–10 keV luminosity (the K -correction accounts for the redshift dependence of the luminosity in a given band of wavelengths). Error bars show 90% confidence. Times are referred to the BAT trigger. Rest-frame time is obtained by applying correction factor $(1+z)^{-1}$ to the observer frame time. Gaps in XRT-PC data correspond to the part of the orbit when the satellite was not observing this GRB. Bottom, change in photon index (Γ , defined by the power law $F(E) = E^{\Gamma+1}$, where $F(E)$ is the observed flux of energy E) of GRB 050904 during the observation. Spectra were modelled using a power law with two absorbing components (galactic and intrinsic).

1. MacFadyen, A. I., Woosley, S. E. & Heger, A. *Astrophys. J.* **550**, 410–425 (2001).
2. Tagliaferri, G. *et al. Astron. Astrophys.* **443**, L1–L5 (2005).
3. Kawai, N. *et al. GCN Circ.* 3937 (2005).
4. Becker, R. H. *et al. Astron. J.* **122**, 2850–2857 (2001).
5. Gehrels, N. *et al. Astrophys. J.* **611**, 1005–1020 (2004).
6. Sakamoto T. *et al. GCN Circ.* 3938 (2005).
7. Mineo, T. *et al. GCN Circ.* 3920 (2005).
8. Burrows, D. N. *et al. Science* **309**, 1833–1835 (2005).
9. Zhang, B. *et al. Astrophys. J.* (in the press); preprint at <<http://arXiv.org/astro-ph/0508321>> (2005).
10. Nousek, J. A. *et al. Astrophys. J.* (in the press); preprint at <<http://arXiv.org/astro-ph/0508332>> (2005).
11. Bromm, V. & Loeb, A. *Astrophys. J.* (in the press); preprint at <<http://arXiv.org/astro-ph/0509303>> (2005).

Competing financial interests: declared none.

Received 11 November 2005; accepted 23 November 2005.
doi:10.1038/440164a

CORRIGENDUM

Developmental technology: Dogs cloned from adult somatic cells

Byeong Chun Lee, Min Kyu Kim, Goo Jang, Hyun Ju Oh, Fibrianto Yuda, Hye Jin Kim, M. Hossein Shamim, Jung Ju Kim, Sung Keun Kang, Gerald Schatten, Woo Suk Hwang
Nature **436**, 641 (2005)

Supplementary Table 1 of this communication has been replaced (9 March 2006; corrections shown in red) as the original peak values reported for two of the canine microsatellite markers (PEZ02, REN105L03) were in error; also, those for PEZ08 have been removed (further details are available from B.C.L. at bclee@snu.ac.kr). In the Table legend, the URL giving details of the markers has been updated. The patent application mentioned in the legend should originally have been declared as a competing financial interest.
doi:10.1038/440164b

BRIEF COMMUNICATIONS ARISING online
♦ www.nature.com/bca see *Nature* contents.

BRIEF COMMUNICATIONS

An accessory chromophore in red vision

The rods in salamanders' retinas can co-opt a molecule derived from chlorophyll to detect red light.

In the absence of a red-sensitive visual pigment, some deep-sea fish use a chlorophyll derivative in their green-sensitive rod cells in order to see deep-red light^{1–3}. Here we show that living rods extracted from a salamander can also accumulate an exogenous chlorophyll derivative, chlorin *e*₆, that renders them as sensitive to red light as they are to green. This vision enhancement by an unbleachable chlorophyll derivative might therefore be a general phenomenon in vertebrate photoreception.

The outer segments of rod cells are rich in rhodopsin: this visual pigment consists of retinal, a form of vitamin A that isomerizes when it absorbs light, and opsin, a protein that changes shape in response to retinal isomerization, which triggers a signal.

We measured the absorbance spectra of individual rods from tiger salamanders (*Ambystoma tigrinum*) by microspectrophotometry (for methods, see supplementary information). Absorbance peaked at wavelengths of 520 nm and 278 nm, owing to the retinal chromophore and the opsin, respectively.

When rods were preincubated with chlorin (Fig. 1a), we found that chlorin targeted the rhodopsin-laden outer segments of the rods; it increased absorbance at 278 nm, and added peaks at 402 nm and 668 nm (Fig. 1b). The peak at 520 nm was unchanged, so if chlorin did bind to rhodopsin, it did so without influencing the retinal chromophore or the binding pocket that spectrally tunes rhodopsin. The slight increase in absorbance of 278-nm light indicates that chlorin may be perturbing aromatic residues on the surface of rhodopsin.

We selected cells with the highest chlorin content (chlorin:rhodopsin ratio was 0.77 ± 0.22 , mean \pm s.e.m.; $n = 3$) to examine chlorin's effect on rhodopsin's sensitivity to light, measured by its bleaching rate. The bleaching rate was unchanged at 560 nm, a wavelength absorbed well by rhodopsin but poorly by chlorin. However, it was accelerated 180-fold at 668 nm, where chlorin absorbs strongly but rhodopsin absorbance is negligible (Fig. 1c).

This bleaching enhancement was tens to

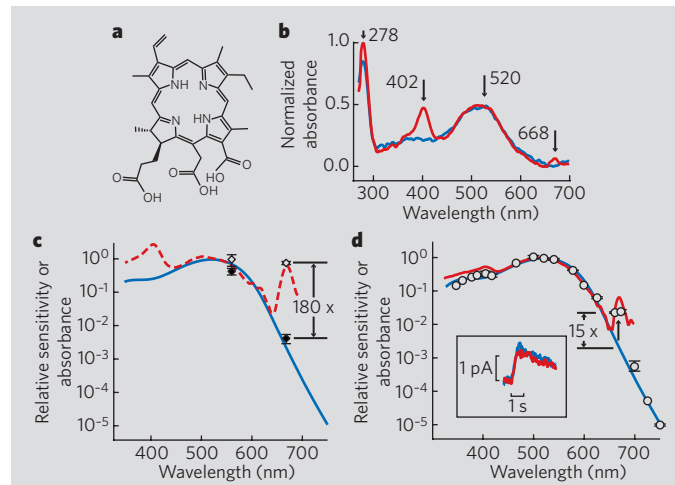


Figure 1 | Chlorin-enhanced response to red light. **a**, Structure of the tetrapyrrole chlorin *e*₆. **b**, Averaged absorption from chlorin-treated (red trace; $n = 5$) and control (blue trace; $n = 5$) rods. The spectrum of treated rods is normalized to the 278-nm peak, and for untreated rods is scaled to match the 520-nm peak for treated rods. **c**, Rhodopsin bleaching from untreated rods (filled symbols; mean \pm s.e.m.), aligned to a template fit⁷ to the spectral sensitivity of seven untreated rods (blue trace). The bleaching rate of rods with high chlorin content (open symbols) is enhanced at 668 nm but not at 560 nm; the rate mirrors the average absorption of such rods (dashed trace), showing that quanta absorbed by chlorin and by rhodopsin are equally effective at bleaching rhodopsin (for details, see supplementary information). **d**, Spectral sensitivity (circles; $n = 3$) increases at 661 and 672 nm in chlorin-treated rods and matches the normalized absorption of a set of rods treated with chlorin and measured microspectrophotometrically (red trace); blue trace is from **c**. Inset, response (in picoamperes, pA) of a chlorin-treated rod to dim flashes at 540 nm (blue; 6.4×10^{-1} photons μm^{-2}) and at 672 nm (red; 22.3 photons μm^{-2}).

hundreds of times greater than the effect of chlorophyll derivatives on dragon fish (*Malacosteus niger*)^{2,3} and bovine⁴ rhodopsins. This shows that chlorophyll-sensitized vision is feasible. Adding 9-*cis*-retinal regenerated a light-sensitive pigment, irrespective of the bleaching conditions that had been used, indicating that chlorin-mediated rhodopsin bleaching was not due to a permanent, photo-induced degradation of opsin (for details, see supplementary information).

In electrical recordings of rods exposed to chlorin, responses to dim flashes were similar in form at all wavelengths (Fig. 1d; inset shows response to two wavelengths). This indicates that photons absorbed by chlorin or by the retinal chromophore directly induce the same active state in rhodopsin. Chlorin treatment increased rod sensitivity to red light (at 661 and 672 nm) by 15-fold (Fig. 1d). This enhancement was less than the 180-fold increase in bleach-

ing rate found earlier, because the cells used for recordings were randomly chosen and contained about 20 times less chlorin (chlorin:rhodopsin ratio, 0.05 ± 0.01 , mode of 61 rods \pm s.e.m.; $n = 15$). Nevertheless, in both microspectrophotometric and electrophysiological experiments, chlorin-assisted bleaching was almost as efficient as direct photoisomerization of the native chromophore (Fig. 1, and see supplementary information).

The mechanism behind the highly efficient energy transfer from chlorin to the retinal chromophore is unclear at this point. However, our results on an amphibian, together with findings from dragon fish^{1–3}, bovine⁴, insect⁵ and prokaryotic⁶ rhodopsins, highlight a potential for spectral enhancement by accessory chromophores in all opsin-based photoreception systems.

T. Isayama*, D. Alexeev*, C. L. Makino*, I. Washington†, K. Nakanishi†, N. J. Turro†

*Department of Ophthalmology, Massachusetts Eye & Ear Infirmary, Boston, Massachusetts 02114, USA e-mail: cmakino@meei.harvard.edu
†Department of Chemistry, Columbia University, New York, New York 10027, USA

1. Bowmaker, J. K., Dartnall, H. J. A. & Herring, P. J. *J. Comp. Physiol. A* **163**, 685–698 (1988).
2. Douglas, R. H. *et al. Nature* **393**, 423–424 (1998).
3. Douglas, R. H. *et al. Vision Res.* **39**, 2817–2832 (1999).
4. Washington, I., Brooks, C., Turro, N. J. & Nakanishi, K. *J. Am. Chem. Soc.* **126**, 9892–9893 (2004).
5. Kirschfeld, K. & Vogt, K. *Vision Res.* **26**, 1771–1777 (1986).
6. Balashov, S. P. *et al. Science* **309**, 2061–2064 (2005).
7. Govardovskii, V. I., Fyhrquist, N., Reuter, T., Kuzmin, D. G. & Donner, K. *Visual Neurosci.* **17**, 509–528 (2000).

Supplementary information accompanies this communication on Nature's website.

Received 4 April; accepted 25 August 2006.

Competing financial interests: declared none. doi:10.1038/443649a

Corrigendum

Developmental technology: Dogs cloned from adult somatic cells
Byeong Chun Lee *et al. Nature* **436**, 641 (2005)

The name of the seventh author on this communication was misspelled. His correct name is M. Shamim Hossein.